

The phases of QCD reached in terrestrial and cosmic colliders

Sourendu Gupta

International Center for Theoretical Sciences, Tata Institute of
Fundamental Research, Survey 151 Shivakote, Hesarghatta Hobli,
Bengaluru North, 560089, India.

Corresponding author(s). E-mail(s): sgupta@theory.tifr.res.in;

Abstract

We review the current state of knowledge of the phase diagram of QCD through lattice, effective field theories, and chiral models. Several sections through the three dimensional phase diagram are known for $N_f = 2 + 1$ with good precision. Due to technical advances in lattice techniques over the last decade or so, new aspects of the phase diagram can now be explored. We review current lattice results. The newly acquired knowledge can be used to reconstruct the full phase diagram for physical QCD, *i. e.*, $N_f = 1 + 1 + 1$. We remark on the computations which would help understand this better, and what the current constraints are on matter in neutron star cores. We also remark on the physics of the chiral transition and neutron stars in the 't Hooft large N_c limit.

Keywords: QCD, phase diagram, heavy-ion collisions, neutron stars

1 The space of the phases of QCD

Although field theoretic foundations for the computation of strong interaction thermodynamics were established long back, there are many challenges in its use. Not only is computing power an issue, but there are also some foundational issues with its use, for example the fermion sign problem. One aim of this work is to review some recent methods and results from lattice QCD computations. A second aim is to use this information and basic thermodynamic arguments to try to constrain the phase diagram of $N_f = 1 + 1 + 1$ QCD. This allows us to address the connection between

Fig. 1 The thermodynamics of a gluon gas has two dimensional Gibbs space labelled by E and S . The phase diagram, shown here, is one dimensional and labelled by T . If there are confined and deconfined phases, then Gibbs' phase rule indicates that the phase diagram has a single first order transition, labeled here as T_d .

heavy-ion collision (HIC) experiments and the properties of neutron stars (NS), and where theoretical methods help to connect the two.

When a system comes to equilibrium all the quantities that describe its changeable character are gone, and only the conserved quantities remain. For strongly interacting matter these are the energy (E), baryon number (B), and its electrical charge (Q). So the thermodynamic description of this matter involves these extensive quantities, along with the entropy (S). This is true whether we consider such matter in the early universe, in extreme astrophysical conditions, or in the lab. Of course, equilibrium does not mean static. At microscopic scales the conserved quantities may move from one constituent to another, but in the coarse grained description that we call thermodynamics, this is irrelevant.

In this four dimensional Gibbs space, states in thermodynamic equilibrium are described by the convex entropy surface $S(E, B, Q)$. A different description of the same surface is given by the function $E(S, B, Q)$. The slopes of this energy surface, *i. e.*, the partial derivatives of this function E with respect to its arguments, defines the thermodynamic intensive quantities T , μ_B and μ_Q . An equivalent description is obtained by working in the space of phases of matter, which is labelled by these intensive quantities.

From E one defines, through successive Legendre transformations, the thermodynamic potential, $\Omega(T, \mu_B, \mu_Q)$. In each distinct phase of matter there is only one continuous and convex function Ω . However, when there are multiple phases, each may have a distinct function Ω . A thermodynamic system always settles into the phase with the lowest Ω . We argue next that the phase diagram can be thought of as a plot of the discontinuities and singularities of the thermodynamic potential as a function of the intensive quantities.

At some points it is possible for two phases, say a and b , to have equal values of the potential. Then we say that the two phases can coexist, or in the old language formalized by Ehrenfest, that there is a first order transition between them. Obviously, with three variables, one equation $\Omega_a(T, \mu_B, \mu_Q) = \Omega_b(T, \mu_B, \mu_Q)$, in general gives two-dimensional surfaces of solutions. So there are surfaces of phase coexistence. Along these surfaces the change in entropy from one phase to another is called the latent heat. When this vanishes the functions Ω_a and Ω_b are no longer distinguishable, and the coexistence surface has come to an end. It can be proved that both Ω_a and Ω_b have a singularity when the latent heat vanishes [1]. This is called a critical point, or in the older language of Ehrenfest, a second order transition. Since two dimensional surfaces end along curves, these edges are critical lines in the phase diagram.

The only other way for a surface of coexistence to end is by meeting another such surface. Again this happens along a line. On this line three phases coexist. If one of

the surfaces also happens to end in a critical line, then the intersection of the critical line with the three phase coexistence line gives rise to a tricritical point. Arguments such as these are Gibbs' phase rules.

The simplest thermodynamic systems are pure gauge theories. Since the only conserved quantity is E , the Gibbs space is two dimensional, with extensive quantities E and S . The space of phases is one dimensional and has the coordinate T , where $dE = TdS$. There may be a single phase in a pure gauge theory, as in the case of pure gauge electromagnetism (EM), *i. e.*, a photon gas. There are no phase transitions. However, non-Abelian pure gauge theories can have two phases: either a confined phase or the non-Abelian analogue of the photon gas. Hence there can be two thermodynamic potentials. As a result, Gibbs' phase rule indicates that there can be a single first order phase transition between these two phases. This is called the deconfinement phase transition.

For $SU(N_c)$ gauge theory with $N_c = 2$ the deconfinement phase transition is of second order [2, 3]. This violates Gibbs' phase rule. One notes however, that the order parameter for deconfinement is related to the free energy of a quark. A quark coupled to $SU(2)$ gauge theory has an extended symmetry compared to any other number of colours, N_c . This prompts us to examine the phase diagram of pure gauge theories as a function of both T and the theory parameter N_c . In this plane, there is a line of first order phase transitions for $N_c > 2$ [4] which ends in a critical point at $N_c = 2$. This is completely compatible with Gibbs' phase rule. In fact we also have the "prediction" that a photon gas has no phase transition. What we learn from this is that apparent violations of the Gibbs' phase rule are possible, and are due to enhanced symmetries. In that case one has to investigate a theory parameter which breaks the symmetry generically. It is interesting that thermodynamics predicts these topological features of the phase diagram of non-Abelian pure gauge theories without any reference to the microscopic physics.

Matter at high temperature or density in nature is not made solely of strongly interacting particles. Photons and neutrinos in the early universe may be an important part of the mixture. Stability over macroscopic distances also requires local charge neutrality. Departures from this condition will result in internal currents in matter which eventually restore the neutrality and bring the system back to equilibrium. In such mixed systems consideration of the conserved lepton number may be needed.

In HICs the huge separation of time scale between the strong and weak interactions means that strangeness may be considered to be conserved in the strongly interacting fireball. A full description of the corresponding thermodynamics would then require us to take into account the net strangeness, and the conjugate intensive variable, namely the strangeness chemical potential μ_s . Such a four dimensional phase diagram may also be relevant in neutron stars (NSs) where stability against beta-decay may be achieved with a large strangeness density [5]. However, studies in this full four dimensional space are very limited, and we will consider the slice with $\mu_s = 0$, since this seems to suffice for HICs and many NSs.

This completes a list of the interesting dimensions of the phase diagram of strongly interacting matter. There are also parameters in the QCD Lagrangian, namely the quark masses, m_u , m_d and m_s . They are tuned non-perturbatively to reproduce known

meson and baryon masses. However, in order to understand the phase diagram, we have to understand the effect of chiral symmetry of QCD when one or more masses vanishes: this is chiral QCD. Then it is convenient to study QCD by changing the quark masses. So the theoretical space of phases contains three more dimensions (the quark masses) than the phase diagram. For example, one particular section of the theory space ($m_\ell = m_u = m_d$, $\mu_B = \mu_Q = \mu_S = 0$), namely the Columbia plot, has long been studied for the insights it provides into the problem [6, 7]. One major result is that the topology of the phase diagram is extremely insensitive to m_s , provided that the pion mass is not ultralight (much lighter than the physical value) or ultraheavy (much heavier than physical).

It is common to use the notation $N_f = 3$ for the slice $m_u = m_d = m_s$, and $N_f = 2 + 1$ for $m_u = m_d < m_s$. The breaking of $N_f = 3$ to $N_f = 2 + 1$ is accomplished by tuning the light and strange quark masses, m_ℓ and m_s , in order to reproduce the isospin averaged values of the meson masses m_η , m_K , and m_π . We will also discuss chiral QCD, for $N_f = 2 + 1$ this has $m_\pi = 0$ but the other mesons have non-vanishing mass. The physical theory is QCD with $N_f = 1 + 1 + 1$. Breaking $N_f = 2 + 1$ to $N_f = 1 + 1 + 1$ would entail tuning the difference between d and u quark masses, Δm , in order to further reproduce the physical value of $m_{\pi^0}^2/m_{\pi^\pm}^2$. Since part of the difference in masses of charged hadrons and their uncharged isospin partners is due to electromagnetic (EM) effects, this tuning is quite finicky. So it is interesting to examine the topology of the phase diagrams with changing Δm to see whether it is sensitive to this parameter.

In various situations of interest, either in NSs or in HIC experiments, strongly interacting matter may be immersed in large external magnetic fields, B . In such cases the influence of magnetic field on the phase diagram may be of interest. The energy density of strongly interacting matter is controlled by a scale close to the pion mass, m_π . Clearly $B \simeq \mathcal{O}(m_\pi^2)$ is necessary for magnetic fields to influence strong thermodynamics. Magnetic fields as large as these could be produced momentarily in the very early stages of HICs, but there is no clear evidence that such large fields persist until matter is thermalized. In astrophysics, the largest magnetic fields, as much as 10^{15} Gauss, are found in magnetars. However, 10^{15} Gauss = $10^{-3}m_\pi^2$, so the change in the phase diagram due to such magnetic fields is expected to be minimal. In this review we will ignore this effect (see [8] for a recent review of developments).

Other theory parameters can also be tuned. QCD-like theories with different number of colours, N_c , have been studied [9–12]. As long as the conserved global quantities are the same, their study can throw light on QCD. Recently interesting new aspects of QCD phases have been found when N_f and N_c are varied simultaneously [13]. Also of deep theoretical interest is the question of how the broken axial $U(1)$ symmetry of QCD affects thermodynamics and the phase diagram [14–16]. Among lattice techniques, there have been advances [17, 18] in the method of differential reweighting [19] by a Taylor expansion of the quark determinant inside the path integral. Discussion of these questions lie outside the scope of this review. The technique of Functional Renormalization Group [20–22] has recently been used for QCD [23]. This subject requires a separate review.

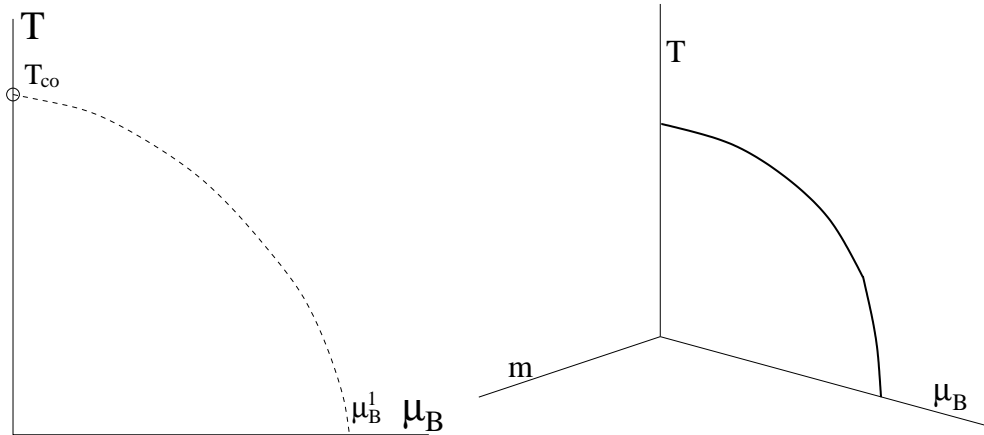


Fig. 2 The most parsimonious phase diagram for QCD with $N_f = 2 + 1$ based on current lattice results and experiments. At fixed and non-vanishing pion mass it would yield only a crossover (panel on the left). An estimate of μ_B^1 , where the crossover line crosses the axis is given in the text. This is a shadow of a critical line in the chiral limit, with a measured curvature (panel on the right). This critical line bounds a surface in chiral QCD at which different signs of S coexist.

2 The T - μ_B plane

The part of the phase diagram of strongly interacting matter that can be probed in relativistic heavy-ion collisions has large variations in T and μ_B and relatively small variations in μ_Q . Lattice computations suffer from a sign problem when $\mu_B \neq 0$ is introduced into the QCD action, but are able to give accurate and precise information for $\mu_B = 0$. Taylor expansions of thermodynamic variables can then be used to extrapolate to finite μ_B . We examine the situation with $\mu_B = 0$ before moving on to the rest of the phase diagram. In these arguments the relevant order parameter is the quark condensate $\mathcal{S} = \langle \bar{\psi}\psi \rangle$. Its value distinguishes between the hadron phase, where $|\mathcal{S}|$ is large, and the quark phase, where it is small, and vanishing in chiral QCD.

2.1 Lattice results

It has been known for a long time that there is no phase transition in QCD with two light flavours and one heavy flavour (strange) of quarks [6, 7, 24, 25]. Instead of a discontinuous or singular behaviour of thermodynamics at a phase transition, one has a continuous change of behaviour. However it is abrupt enough to give interesting experimental signals. This is a cross over—the speed of sound may go through a non-zero minimum at one temperature, a susceptibility can have a non-singular peak at another temperature T_{co} , etc. The temperature interval where such extrema occur has a non-zero width ΔT . Different maxima and minima can occur anywhere in this interval.

In chiral QCD then there is second order transition [24]. Since μ_B does not affect the symmetry which is broken or restored across T_c , this critical point develops into

a critical line, which can be parametrized at small μ_B as

$$T_c(\mu_B) = T_c \left[1 - \kappa_2 \left(\frac{\mu_B}{T_c} \right)^2 - \kappa_4 \left(\frac{\mu_B}{T_c} \right)^4 + \dots \right], \quad (1)$$

where we used the notation T_c for the more cumbersome $T_c(\mu = 0)$. The coefficients κ_2 and κ_4 are called curvature coefficients. Flipping quarks with antiquarks is equivalent to $\mu_B \leftrightarrow -\mu_B$, and the flip does not change any physics. That's why the expansion in eq. (1) contains only even powers of μ_B .

Many modern day computations of thermodynamics are performed with improved staggered quarks with two degenerate light flavours and a somewhat heavier flavour (strange). The improvement consists of control over lattice spacing effects, so that continuum extrapolations are straightforward. Bare quark masses are tuned to reproduce the mean masses of isospin multiplets of the pseudoscalar SU(3) flavour octet mesons properly. Two sets of extensive computations for the phase diagram can be compared. These are results at finite T and vanishing charges and external fields

$$T_{co} = 156.5 \pm 1.5 \text{ MeV}, \quad \kappa_2^B = 0.015(4), \quad \kappa_2^Q = 0.027(4), \\ \kappa_4^B = -0.001(3), \quad \kappa_4^Q = 0.004(5), \quad (2)$$

from [26]. Here $\kappa_{2,4}^Q$ are curvatures in the μ_Q direction. These results are statistically consistent with those from [27],

$$T_{co} = 158.0 \pm 0.6 \text{ MeV}, \quad \Delta T = 15 \pm 1 \text{ MeV}, \\ \kappa_2 = 0.0153(18), \quad \kappa_4 = 0.00032(67) \quad (3)$$

It is instructive to note that although a particular measurement of T_{co} can be made more and more precise through more statistics and by careful control of various systematic errors, the width of the cross over region, ΔT is expected to remain non-vanishing. The most parsimonious phase diagram with all these inputs is shown in Figure 2. It is compatible with old expectations that followed from [24].

The lattice determinations of T_{co} for varying quark masses have been extrapolated to chiral QCD using the scaling exponents for the flavour symmetry group $SU_L(2) \times SU_R(2) \simeq O(4)$. This gives [28]

$$T_c = 132_{-6}^{+3} \text{ MeV}. \quad (4)$$

In all the results quoted here, lattice spacing effects are under good control. Reliable simulations are now available at quark masses which are not only realistic, but also for masses lower than physical. This improves the reliability of the extrapolation to chiral QCD.

A new generation of simulations of thermodynamics with improved Wilson quarks has started [29, 30], but the pion masses which are accessible are generally higher. Still, one can look forward to better quantification of the effects of lattice spacing by a comparison of two different methods of putting quarks on the lattice. Most simulations

use a spatial lattice volume which is pretty large. However, in future one should look forward to a proper finite size scaling study if the cross over, especially in order to control the extrapolation to chiral QCD as the quark mass is decreased below the physical mass

2.2 Effective field theory

Chiral symmetry has been used in various ways before. Famously, the NJL model has been used to understand the effects of this symmetry, and has been found to be numerically fairly accurate for several kinds of quantities [31]. More importantly, at $T = 0$ an effective field theory (EFT) called chiral perturbation theory (χ PT) is known to work extremely well [32] (see also [33]) for low energy hadron physics. Its success has prompted lattice computations at $T = 0$ to concentrate on precision measurements of amplitudes which constrain the parameters of χ PT. the EFT is then used to compute amplitudes which are hard to access using lattice methods. χ PT has also been extrapolated to finite temperature [34, 35], albeit with less success.

Recently the NJL model has been generalized to a thermal EFT by adding all possible terms which are allowed by symmetry (apart from flavour symmetry one also incorporates the broken Lorentz invariance for $T > 0$), and organized by the scaling dimension (D) of operators. Keeping all the operators up to $D = 6$, one can find a good description of lattice measurements of static properties of pions using only three pieces of data from lattice computations to fix the low-energy constants (LECs) [36]. Hartree-Fock treatment of this theory one can recover a finite temperature analogue of χ PT.

Interestingly if one fits only pion properties at $T \geq 0$ for $N_f = 2 + 1$ QCD then the phase diagram can be recovered quantitatively from the EFT [37]. One finds T_{co} , κ_2 and κ_4 in excellent agreement with eq. (2) and eq. (3) within 68% confidence limits (CL). The relatively large errors in lattice measurements of the curvatures is the weakest quantitative test of the lattice at present. halving the errors in the lattice measurement of κ_2 would test the accuracy of the EFT quite stringently. In the limit of chiral QCD, T_c from the EFT is also in agreement with [28].

The EFT can also give results which are currently impossible to obtain from the lattice. One such is the pole mass of pions at finite temperature. The difference between screening and pole masses is a direct consequence of thermal effects, and is captured in an EFT through the fact that broken Lorentz symmetry (in the Euclidean theory) allows the kinetic term in the pion Lagrangian to become

$$\frac{1}{2}(\partial_\mu \pi)^2 \xrightarrow{T>0} \frac{1}{2}(\partial_t \pi)^2 + \frac{1}{2}u_\pi^2(\nabla \pi)^2. \quad (5)$$

In chiral QCD the pole mass, m_π , vanishes for $T < T_c$ and u_π drops to zero at T_c with a critical exponent [38] Using the pion propagator from eq. (5) one finds the Debye screening mass $m_\pi^D = m_\pi/u_\pi$. The EFT for $N_f = 2 + 1$ predicts that when the $T = 0$ pion has mass of 140 MeV, the pole mass drops to about 110 MeV at $0.85T_{co}$ and to about 100 MeV at T_{co} . Lattice measurements show that m_π^D increases faster than linearly with T for $T \simeq T_c$. This is due to the fact that the physical pion mass is

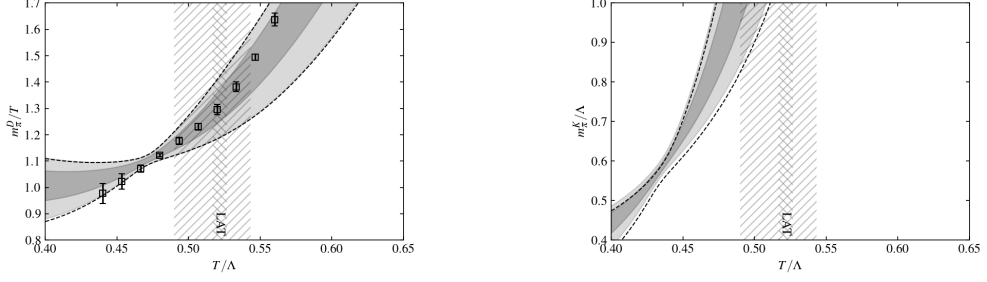


Fig. 3 The panel on the left shows that the screening mass of the pion, m_π^D , is found to be continuous across T_c in lattice computations. The data points show continuum extrapolated results from the lattice. This is reproduced well by the EFT (dark shading for the 68% error band, light shading for the 95% error band), which has a UV cutoff Λ . This particular fit uses $\Lambda = 300$ MeV, but equally good fits are obtained using $\Lambda = 450$ MeV. The vertical hatched band shows T_{co} (the narrow band is from the lattice, the wider band from the EFT). The panel on the right shows the kinetic mass, m_π^K . Since it becomes comparable to Λ at about T_{co} , pions are no longer the low-energy excitations of QCD.

close enough to vanishing that u_π drops near T_{co} although it does not vanish. Due to this behaviour of u_π , the pressure, P/T^4 , also shows a rapid rise near T_{co} . However, it seems that NLO terms in thermal χ PT are likely to be needed in order to give a quantitative description of the pressure below T_{co} .

The Minkowski version of the model Lagrangian in eq. (5) then shows that the energy of a pion of 3-momentum p is

$$E_p = m_\pi + \frac{1}{2} \frac{p^2}{m_\pi^K}, \quad (6)$$

where the kinetic mass $m_\pi^K = m_\pi/u_\pi^2$. Since u_π decreases towards T_{co} , one sees that m_π^K increases [39]. As a result, pion gains energy more slowly with increasing p close to T_{co} than it would have at a lower temperature. This would close off certain inelastic reactions as one approaches T_{co} .

Through this mechanism the EFT helps us to untangle the specific physics of the QCD crossover. The continuity of screening masses across T_{co} has been known for a long time. It is reproduced well by the EFT, as shown in Figure 3. This means that appropriate probes can pick out pions in hot matter. However, the kinetic mass of the pion rises rapidly, showing that as far as dynamical processes are concerned, the pion can no longer be considered a light collective mode near T_{co} . Other fluctuations of quarks must then be investigated. The presence of static pions and its simultaneous absence from dynamics is one aspect of QCD that lattice computations presumably contain, but which can be made explicit only after Wick rotation. The EFT is an effective tool for this.

2.3 The physical phase diagram

The structure of the phase diagram of $N_f = 2 + 1$ QCD with realistic meson masses is conjectured on the basis of effective theories [40–42]. Only the order parameter \mathcal{S} is involved in Figure 4. There is a critical line in chiral QCD which stretches from T_c at

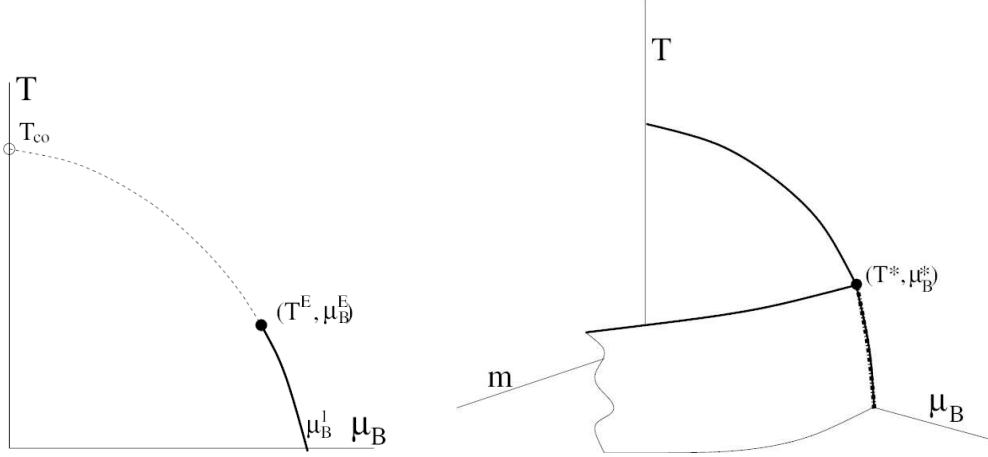


Fig. 4 The conjectured phase diagram for $N_f = 2 + 1$ QCD with a finite quark mass (panel on the left). The crossover at $\mu_B = 0$ develops into a line of crossovers which turns into a line of phase coexistence (a first order transition between hadron and quark phases) at the critical point (T^E, μ_B^E) . When extended in quark mass (panel on the right), the critical point turns into a critical line, which is the boundary of a surface of hadron-quark phase coexistence (part of it is cut away to show the structure). This critical line meets the chiral critical line at the tricritical point (T^*, μ_B^*) , which is the end point of a triple line in QCD. The shape of this phase diagram is not expected to change in $N_f = 1 + 1 + 1$. However, T_{co} , μ_B^1 , and (T^E, μ_B^E) could shift.

$\mu_B = 0$ to the tricritical point, (T^*, μ_B^*) . This critical line is the boundary of a surface of first order transitions between $\mathcal{S} < 0$ for $m > 0$, and $\mathcal{S} > 0$ for $m < 0$. The tricritical point is the end point of a triple line where the three coexisting phases are the two chiral symmetry broken hadron phases, and the third is the chiral symmetry restored quark phase with $\mathcal{S} = 0$. Although the phase diagram of Figure 2 is compatible with all data till now, there are large portions of the phase diagram which have not been studied and could yield evidence for the alternative discussed here.

If first order transitions do occur at finite quark mass, then the critical point, (T^E, μ_B^E) , must lie on the cross over line starting at T_{co} with curvatures which are well determined. The earliest lattice computations for finite μ_B which used Padé approximants found the end point [43] at $\mu_B^E/T^E = 1.85 \pm 0.04$ and $T^E/T_{co} = 0.94 \pm 0.1$. This lies squarely on the cross over curve determined by the parameters in eq. (3) and eq. (2). More recent computations using multi-point Padé [44] report $T^E = 105^{+8}_{-18}$ MeV and $\mu_B^E = 422^{+80}_{-35}$ MeV. This is also compatible with the shape of the cross over curve at $\mu_B = 0$. Interestingly, this work also reported a value of κ_2 at the end point which is in agreement with that at $\mu_B = 0$.

This observation is an useful estimate for a quantitative determination of the coexistence surface between the hadron and quark phases. The values in eq. (2) and eq. (4) predict that for chiral QCD the surface reaches $T = 0$ for $\mu_B = 1100 \pm 150$ MeV. Using the same logic, the first order line at physical meson masses ends at $\mu_B^1 = 1280 \pm 170$ MeV for $T = 0$ using the values in eq. (2). Using eq. (3) we find that $\mu_B^1 = 1280 \pm 75$ MeV.

The phase diagram for realistic pion and kaon masses does not change qualitatively between $N_f = 2$ and $N_f = 2 + 1$, although T_{co} changes in value as the strange quark mass is changed [45]. For physical QCD, *i. e.*, with $N_f = 1 + 1 + 1$ and realistic pion and kaon masses, the phase diagram is not expected to change qualitatively. It is possible however that T_{co} , the curvature coefficients of the cross over line, the location of the end point, and μ_B^1 may change somewhat. The only investigation of $N_f = 1 + 1$ QCD [46] reported that no change in T_{co} was observed when changing the ratio $m_{\pi^0}^2/m_{\pi^\pm}^2$ between unity and 0.78 by changing Δm . It would be useful to bring modern techniques and improved statistics to bear not only on T_{co} but also the curvature coefficients in physical QCD.

If other order parameters are involved at such low T and for such μ_B , for $N_f = 1 + 1 + 1$ QCD, then the physical phase diagram may be more complicated than what is shown here. However, at this time there is no clear evidence for such complications. At very low temperatures, where bound nuclei can exist, interesting phases of nuclear matter are seen. Temperatures as low as a few MeV are therefore outside the scope of these discussions. In this discussion we have also assumed that at μ_B^1 the baryon density is not high enough for colour superconducting (CS) phases to manifest, an assertion which must be tested by other means.

3 The μ_Q - T plane

The electric charge of a system is a conserved quantity which is easy to measure in experiments, so μ_Q is an useful quantity to consider. However, most of the literature instead uses the chemical potential, μ_I , connected to the isospin projection I_3 . Fortunately the Gell-Mann-Nishijima relation $I_3 = Q - (B + S)/2$ allows us to relate the two. It shows that changes in Q and I_3 are equal at fixed B and S . Then equating the energy change due to such fluctuations in the two ensembles implies that $\mu_I = \mu_Q$.

When the u and d flavours of quarks are degenerate in mass, then an isospin chemical potential breaks the SU(2) vector symmetry remaining after chiral symmetry breaking into the U(1) symmetry generated by τ_3 . A computation in a chiral model showed that a pion condensate, \mathcal{P} , forms at $\mu_I = m_\pi/2$ [47]. The model computation showed that the phase transition from the normal hadron to this pion condensed BEC (π C) phase is of second order, and that there is a critical line that emerges from it. Since the remnant symmetry is U(1) \simeq O(2), the critical indices are expected to be in the same universality class as that of O(2) Heisenberg ferromagnetism.

$N_f = 2 + 1$ QCD computations on the lattice with $m_\pi \simeq 135$ MeV [48], show a line of phase transitions starting at $\mu_I = m_\pi/2$. The line is vertical within statistical errors until it meets the line of cross overs between the hadron and quark phases, and is subsequently nearly horizontal. This change of slope occurs at $T \simeq 155$ MeV, but this temperature is uncertain by about 5 MeV. All this is consistent with the quantities reported in eq. (2) and eq. (3). A limited finite volume scaling has been performed to check that the transition line is consistent with the expected O(2) critical transitions. In a follow-up computation [49] it was shown that the speed of sound $c_s > 1/\sqrt{3}$, deep in the π C phase of pionic matter.

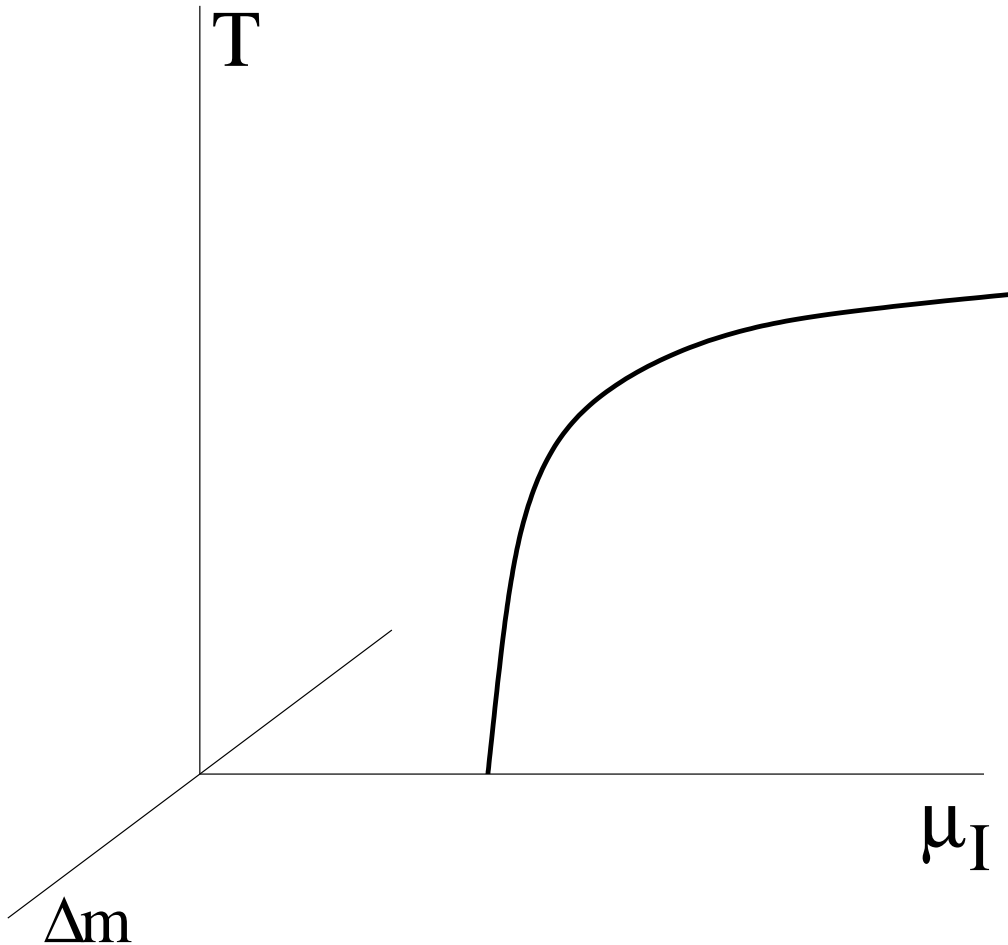


Fig. 5 The phase diagram for $N_f = 1 + 1 + 1$ QCD in the space of T and μ_I as Δm is varied. For $\Delta m = 0$ lattice computations indicate that the critical line between the hadron and π C phases is nearly vertical, until the cross over between the hadron and quark phases is reached. Beyond this the critical line is either horizontal or rises slowly. For any finite Δm the transition turns into a crossover. Since this whole volume has an extended symmetry, an isolated critical line is allowed; this is the edge of a first order surface for a hidden parameter, as explained in the text.

An interesting aspect of these lattice simulations is that a “twisted mass” is introduced in the light quark sector to stabilize the flavour of the pion condensate [50]. The Dirac operator commutes with the flavoured transformation $\tau_2 \gamma_5$ even when the symmetry is broken in this way, so that the determinant remains free of the sign problem. At finite λ the coset space is “tilted” to produce a preferred direction for the condensate, so there is no Goldstone mode. This twisted mass parameter, λ , must be extrapolated to zero to obtain the correct physics of the Goldstone boson in the chiral limit of $N_f = 1 + 1 + 1$. However, Goldstone physics appears as vanishing singular values of the Dirac operator which develop as $\lambda \rightarrow 0$. Even for small non-zero λ they

lead to a large condition number and critical slowing down of the simulation. In [48] the problem is partly resolved by treating the developing zero-modes separately. Using this, a clever separation of the contribution of some of the developing zero and the rest of the modes is used to define a better behaved operator and partially circumvent the problem with the extrapolation to $\lambda = 0$. Several of the techniques used have matured only in the last decade, enabling modern computations to overtake the state of the art in [50].

Instead of $N_f = 2+1$ if one examines the physical theory with $N_f = 1+1+1$, then Δm also breaks $SU(2)$ of isospin to the $U(1)$ generated by τ_3 . Since exactly the same symmetry is broken by μ_I , switching this on in QCD with non-vanishing Δm does not break an existing symmetry, and so cannot produce a critical point. This implies that there is only this line of second order phase transitions in the phase diagram of physical QCD. This is not consistent with Gibbs' phase rule. However, physical QCD still has an unbroken symmetry since there remains one massless mode. The parameter λ breaks this symmetry. The critical line at $\lambda = 0$ is the boundary of a first order region that arises for generic values of these parameters when Δm and μ_I are tuned appropriately. Although this parameter vanishes in QCD, it must be considered as one of the theory parameters of the phase diagram, on the same footing as m and Δm as far as the thermodynamics is concerned.

In this way we understand that the phase diagram of QCD in the Δm - μ_I - T space, shown in Figure 5, is a space with an unbroken symmetry, and hence allows the existence of a critical line without a visible phase coexistence region. Interestingly, when the vector symmetry is broken by Δm , then there is a sign problem for lattice simulations at finite μ_I . Making a Taylor expansion of the free energy [51, 52], but now in μ_I , is an available method that is yet to be applied to this case.

Near any second order transition one can resolve Ω into a singular and a regular piece. The contribution to the specific heat, c_V , considering both pieces near the critical temperature T_c , when μ_I is also tuned to criticality, gives

$$c_V = A + \frac{B}{T_c |T - T_c|^\alpha}, \quad (7)$$

where A comes from the regular piece and B and α come from the universal singular piece [53]. Notice that B can be negative as long as c_V is positive. In fact, microgravity experiments with liquid He [54] show that this is so at the λ -point of He, where the critical behaviour is in the $O(2)$ universality class. Since the universal quantities found in liquid He are $\alpha \simeq -0.012$ and $B < 0$, one may expect the same behaviour in QCD at finite μ_I . This means that c_V is dominated by the regular part of Ω , and it would be hard to see a crossover using thermal properties either in heavy-ion collisions or in neutron star interiors.

A recent lattice computation performed for finite μ_I and T close to zero, for the first time found non-perturbative evidence for a colour superconducting (CS) gap, Δ , at the quark Fermi surface for $\mu_I \geq 1500$ MeV [55]. The computation used closer improved Wilson quarks and an improved gauge action with pions which were not too far from their physical mass. This study also brought together several techniques which have matured only in recent years, and enabled a first look at this exciting and

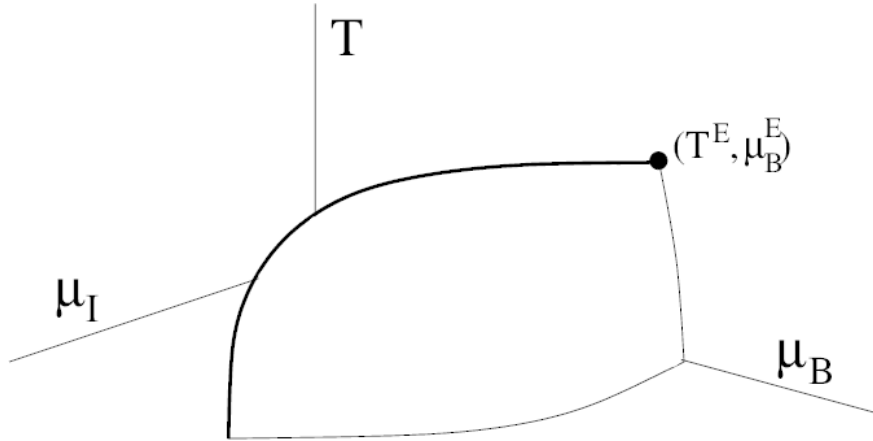


Fig. 6 The conjectured phase diagram of physical QCD for $\mu_S = 0$, based on currently available results from lattice QCD. There is a phase coexistence surface separating the hadron and quark phases which ends along a critical line. This curves down to meet the $T = 0$ plane at the cold critical point (CCP). This accommodates the strong possibility that there is a continuity between the hadron and colour superconducting phases.

long open problem. The evidence for CS came in the form of a disagreement between the pressure estimated on the lattice and a gapless NNLO weak-coupling estimate. In the range 1500–3000 MeV, Δ was found to be roughly 300 MeV or lower (at the upper end of the range Δ was consistent with zero). In this range of μ_I a perturbative estimation of Δ [47] is consistent with the lattice result. There is a systematic trend which needs to be investigated further: the perturbative estimate of Δ increases with μ_I whereas the lattice estimate is either constant or decreasing. A follow up is also needed to check whether Δ remains non-zero till $\mu_I = \mu_I^1 \simeq 1000$ MeV.

4 The phase diagram of physical QCD

Enough information is available now from lattice simulations to patch together the full phase diagram of physical QCD, *i. e.*, QCD with $N_f = 1 + 1 + 1$. Various caveats about the pieces which go into this have been mentioned already, but we bring this list together again. At very low temperatures and μ_B between about 900 MeV and μ_B^1 , there are likely to be interesting phases of nuclear matter. These range from superconducting phases due to pairing forces between nucleons [56] and crystalline structure [57] at the low-density end to nuclear pasta phases [58–60] towards higher densities. There is a gap in the literature regarding the structure of these phases at high μ_I . This is clearly an area ripe for quick exploration. At temperatures below about 100 MeV and around μ_B^1 there is a possibility of encountering colour superconducting (CS) phases [61–63]. If they exist at these μ_B and μ_I , they would definitely affect the boundaries of the quark phase. In view of the current uncertainties regarding the boundaries of these interesting phases, we first present a construction that ignores them, before speculating on how they can affect the tentative conclusions that could be obtained in this way.

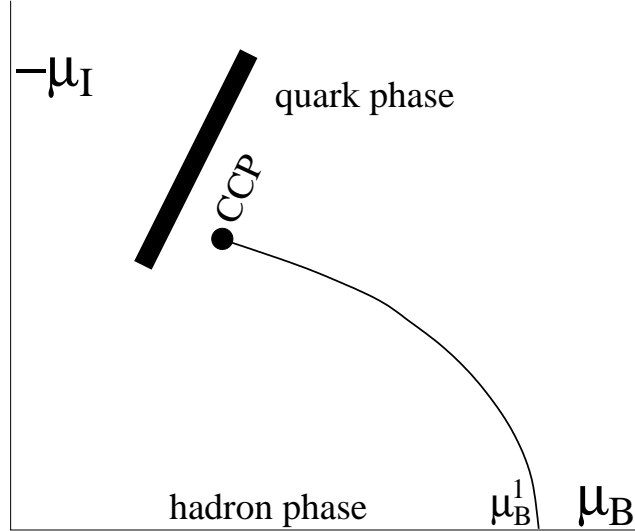


Fig. 7 The phase diagram for NSs at low T which follows from Figure 6. The possible equilibrium states that cores of NSs can explore is shown by the diagonal box. The upper end of the box corresponds to a little over twice the normal nuclear density, and the lower end is the normal nuclear density. We assumed that the CCP lies at larger μ_B than is explored by NSs so that the transition between hadron and quark matter in NS cores is continuous and does not involve a latent heat. This assumption remains to be tested.

We have considered two order parameters: one is the quark condensate \mathcal{S} which distinguishes the hadron and the quark phases, the other is \mathcal{P} , the pion condensate which distinguishes the hadron and π C phases. Current thinking is that that in the plane T - μ_B there is a first order line with phases distinguished by \mathcal{S} . By Gibbs' phase rule, this must develop into a surface in the phase diagram of T - μ_B - μ_I . An alternative is the parsimonious scenario in which there is no first order phase transition for physical QCD in this plane. Heavy-ion collisions might be able to distinguish between these scenarios unless, unluckily, the critical point exists but at too large a value of μ_B/T to show up in experiments. In the T - μ_I plane for physical QCD there is either a mild crossover between the hadron and π C phases, or no crossover at all. We have argued that the crossover, if it exists, may be hard to detect.

The hadron-quark (HQ) coexistence surface touches the μ_B axis at μ_B^1 . The sign of the curvature κ_2^Q in eq. (2) indicates that if this were the only coexistence surface in the phase diagram, then it would meet the μ_I axis at about 900 MeV. So the HQ surface must bend towards the μ_I axis. The question of whether the hadron-quark coexistence surface meets the μ_I axis is interesting. Some arguments are given in [47] that π C goes into CS quark matter without a phase transition in $N_f = 2 + 1$ QCD. This is consistent with the observations in [55]. So the balance of evidence now is that the HQ coexistence surface ends before it can meet the $\mu_B = 0$ plane, this time at large μ_I . This means that there is a critical point in the μ_B - μ_I plane for physical QCD at $T = 0$, *i. e.*, a cold critical point (CCP). A resulting parsimonious phase diagram is that the Ising line in Figure 6 bends down to meet the $T = 0$ plane, and is the

only boundary of the HQ coexistence surface. In this case the CCP is in the Ising universality class. In any case, hadron-quark continuity along the μ_I axis needs to be investigated further. A start can be made on the lattice with $\Delta m = 0$. An alternative to the scenario in Figure 6 is that there are no phase transitions at all. This is not yet ruled out.

There are unresolved questions still about the physics when both μ_B and μ_I are non-vanishing. For example, in [49] it was found that for a large range of μ_I the speed of sound exceeds the conformal limit. Does this still happen when $\mu_B > 0$? And with non-vanishing Δm ? Does the speed of sound drop in the vicinity of the O(2) critical line, *i. e.*, at small Δm ? Lattice computations will be hard with two independent sign problems, but EFTs should help to clarify the range of possibilities.

Heavy ion collisions start with nuclei which are reasonably close to isoscalar ($I_3/A = Z/A - 1/2 \simeq 0.1$ for both Pb_{208}^{82} and Au_{197}^{79}), and come closer to isoscalarity in the central region of the fireball. So the equilibrium states reached in these experiments lie on a plane close to vanishing μ_I parallel to the T - μ_B coordinate plane. They could either give evidence to support the existence of the HQ coexistence surface, or give limits on the values of μ_B/T where it can exist. The cores of NSs, on the other hand, are as far from isoscalar as it is possible for a stable system to go. Newly formed NSs have a temperature of about 10 MeV, and they cool to around 100 KeV in about a million years. So at any given age, NS matter explores a plane of small, but non-vanishing, T parallel to the μ_B - μ_I coordinate plane.

The phase diagram in the plane explored by the cores of NSs is shown in Figure 7. The coexistence line between hadron (πC) and quark (perhaps CS) phases could end in a CCP (which we argued before is possibly in the Ising universality class). Since the baryon density in a NS is almost completely due to neutrons, $\mu_I \simeq -2\mu_B$. Neutron star cores lie along this line with μ_B corresponding to somewhere between nuclear saturation density and twice that. Current lattice studies then indicate that the cores are either in the hadron/ πC phase or in a quark phase. Whether this quark phase is CS is not yet determined by lattice QCD. Note that the track followed by the NS core may or may not cross a first order transition depending on the as yet unknown position of the CCP. There is also a chance that there is no HQ coexistence line, and the whole phase diagram is trivial.

In binary NS collisions, when matter is initially heated, it goes out of thermal equilibrium. However, if the result of the merger comes back to thermal equilibrium, then it does so at a higher temperature. Possibly this could be a significantly higher temperature than of order 10 MeV. Also, since the merged object is heavy, it would be at a higher density. As a result, the remnant, whether it eventually becomes a NS or a black hole, could pass through a phase of quark matter, possibly colour superconducting quark matter. Unfortunately, this object is hidden inside a hot cloud of radioactive nuclei synthesized during the collision. Penetrating signals from this merged object are therefore interesting to search for.

It is exciting that in the last ten years or so, lattice studies have begun to constrain the possibilities for the physics at the core of NSs. Many of the conjectures first made about 25 years ago are being tested, and, as discussed here, this leads to new conjectures for the phase diagram of QCD. We have discussed at various places in

this review where lattice, EFT, or model studies can lead to greater constraints on the possible physics. This is an exciting time in the physics of hot and dense strongly interesting matter.

5 Chiral transition and neutron stars at large N_c

Some aspects of strong interactions are simpler to examine in the 't Hooft limit, $N_c \rightarrow \infty$ while holding $g_s^2 N_c$ fixed. It was argued by 't Hooft [66], that in this limit one can use weak-coupling arguments to understand aspects of QCD which are otherwise nonperturbative. In this section we apply this counting to aspects of the QCD chiral transition and to neutron stars. Since the physics of neutron stars involves charge neutrality and stability against weak decays, they cannot be understood within the strong interactions only. The electroweak interactions play an important role. If one wants to take the limit of the number of colours, N_c , to be large while retaining realistic physics, one has to consider the limit in the appropriate extension of the standard model.

We will take the minimal particle content needed, which is two flavours of quarks, and the electron and the neutrino. The chiral symmetry of QCD is then $SU_L(2) \times SU_R(2) \times U_B(1)$. The gauge group is $SU(N_c) \times SU_L(2) \times U_Y(1)$ where Y is the weak hypercharge and we have the usual chiral form of the weak interactions. With just one generation of quarks, global $SU(2)$ anomaly cancellation requires odd N_c . Then with the usual assignment $Y = \pm N_c + 1$ to the u and d quarks and unity for leptons, we find first,

$$Q_u - Q_d = 1, \quad \text{and second,} \quad Q_u^2 - Q_d^2 = \frac{1}{N_c^2} \quad (8)$$

from ABJ anomaly cancellation [64, 65]. We will take the lepton charges to be as usual. However, the mixing amplitude for ρ and γ varies as ef_ρ , where the ρ decay constant $f_\rho \propto \sqrt{N_c}$. In order to keep the amplitude from growing, and hence pushing up the ρ mass, the 't Hooft limit requires the scaling $e^2 N_c \rightarrow \text{constant}$ as N_c is taken to infinity [64]. Similar arguments as N_c is taken to infinity for internal W^\pm and Z lines require the scaling $g_2^2 N_c$ to go to a constant, where g_2 is the electroweak coupling. The only remaining parameters in the Lagrangian are the fermion masses, m , and θ_W , which are both taken to be fixed in the 't Hooft limit. With this, the scalings discussed by 't Hooft [66] and Witten [67] can be recovered.

The flavour multiplets of the mesons are the same as for $N_c = 3$. However, since we build baryons by taking N_c quarks, they can have isospins between $1/2$ and $N_c/2$. In the doublet representation one has the large N_c analogue of the proton with $(N_c + 1)/2$ up quarks and $(N_c - 1)/2$ down quarks, so that its charge is unity. The isospin flipped state has vanishing charge, and is the large N_c analogue of the neutron. As long as the u quark is lighter than the d quark, one can have the β decay $n \rightarrow pe^- \bar{\nu}$. In the large N_c limit the tower of states with equal spin and isospin ($J = I = 1/2, 3/2, 5/2, \dots$) are degenerate, giving an effective $SU(4)$ spin-flavour symmetry which is similar to the quark model [68, 69].

To proceed one needs to examine these baryon masses in QCD. The small current quark mass which appears in the Lagrangian of the Standard Model is often supplemented by a constituent quark mass, m , which is such that the ρ meson mass is about

$2u$ (since quark and antiquark masses are equal), and the nucleon mass is about $3u$. Generalizing this using Witten's counting rule [67] would give us $u \propto N_c^0$. In models of chiral symmetry breaking the constituent masses of the quarks arise from the chiral condensate, $\langle \bar{\psi}\psi \rangle$. Since $m_\pi^2 f_\pi^2 = m \langle \bar{\psi}\psi \rangle$, with $m_\pi \propto N_c^0$ and $f_\pi \propto N_c^{1/2}$, one has $\langle \bar{\psi}\psi \rangle \propto N_c$. In such models one also finds $u \simeq \langle \bar{\psi}\psi \rangle / N_c \propto N_c^0$, which is consistent with the above. This argument implies that quark masses are fixed in some units independent of N_c , and that baryon masses increase when N_c increases. Furthermore, the mass degeneracy that gives SU(4) spin-flavour symmetry is lifted at order $1/N_c$ [70]. For the baryon masses one finds

$$m_B = N_c \left[a_0 + a_1 \left(\frac{J}{N_c} \right)^2 + a_2 \left(\frac{J}{N_c} \right)^4 + \dots \right], \quad (9)$$

with constants a_i to be determined and with the $J = 1/2$ doublet having the lowest mass.

This is a good place to discuss phase transitions at finite temperature. In the chiral limit of QCD, the chiral condensate, $\langle \bar{\psi}\psi \rangle$, is an order parameter for the chiral symmetry restoring phase transition. The phase diagrams of the previous sections have been constructed using this order parameter and related physics. The chiral transition temperature, T_c in eq. (4), is expected to scale as N_c^0 . When the lightest quarks are very massive, then one expects QCD to have a deconfining phase transition, with an order parameter called the Polyakov loop. These considerations are incorporated into the Columbia plot [6], and a deconfining transition temperature $T_d = 192 \pm 4 \pm 7$ MeV was reported in [71]. In [9] it is argued that T_d is expected to scale as N_c^0 . Scaling arguments cannot resolve whether $T_c < T_d$ in the 't Hooft limit. A parsimonious argument about the relationship between these phase transitions was presented in [4] and summarized in Figure 8.

Within the EFT discussed in Section 2 it is possible to construct a large- N_c argument which shows that the curvature coefficient κ_2 is two powers of N_c smaller than T_c and that κ_{n+2} is two powers of N_c down from κ_n . As a result, in the large N_c limit $T_c(\mu_B)$ becomes independent of μ_B . It is interesting to note that both the chiral critical line (in region A of Figure 8) and the first order deconfinement transition line (in region B of Figure 8) are independent of μ_B in the 't Hooft limit. It is also interesting to note that since the baryon mass is of order N_c whereas meson masses are of order N_c^0 , baryonless thermal EFTs may continue to play an important role in the chiral symmetric phase of QCD.

Returning next to the physics of baryons, we see that baryon-baryon interactions which give rise to nuclear physics, as well as interactions of baryons with electrons or photons are subleading in N_c . So, one might find that models of stellar physics simplify in the large N_c limit. However, one has to take the 't Hooft limit in order to ensure that not all stars become black holes. The mass of a star with A nucleons, say the same as the baryon number of the sun, scales as $M_\odot \propto N_c$. The Schwarzschild radius of a black hole with this mass scales as N_c/G_N . In order to leave space for normal stars, this cannot go to infinity as $N_c \rightarrow \infty$. This requires that to take the 't Hooft limit one should scale down the Newton constant by taking $G_N N_c$ to be a constant.

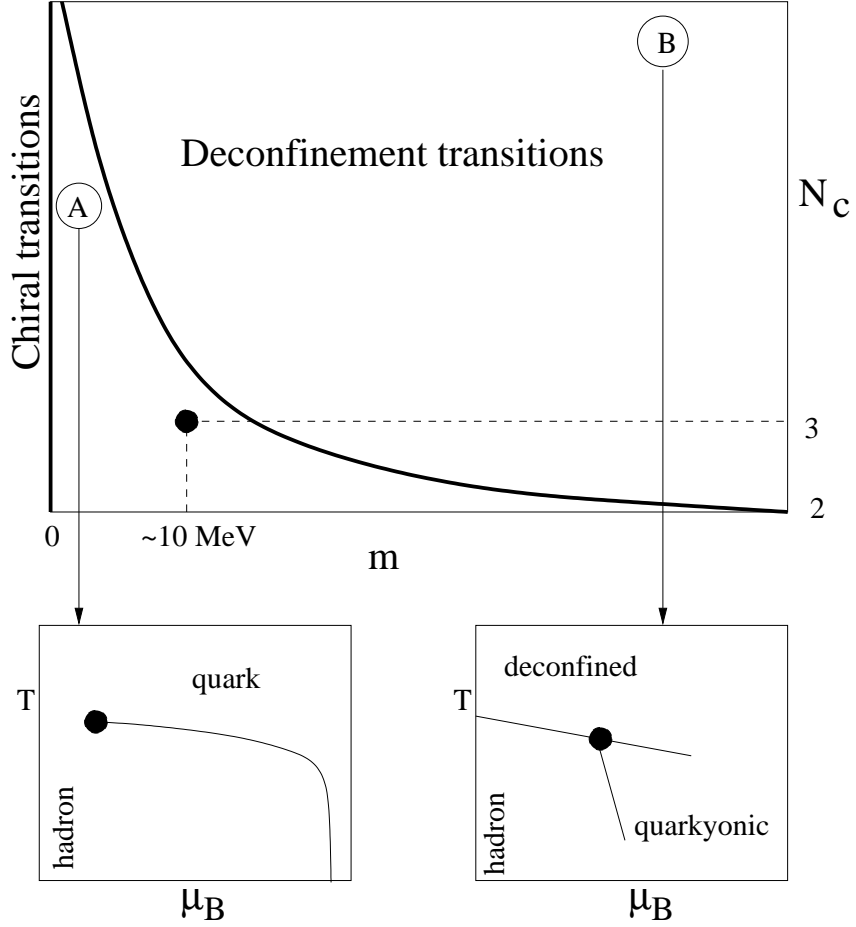


Fig. 8 The most parsimonious model of the relationship between the chiral and deconfinement transitions with changing N_c which follows from our knowledge of $N_c = 3$. The difference between T_c and T_d cannot be resolved through power counting alone. The regions labelled A and B give different phase diagrams, as shown. The phase diagrams that are discussed in the previous sections hold in region A.

By taking the constant to be zero, one can also accommodate a faster decrease of G_N with N_c . Note that the large- N limit used in the AdS/CFT correspondence requires a different scaling $G_N N_c^2$ being held constant. This faster fall of Newton's constant is also compatible with a separation between the radii of black holes and stars in the 't Hooft limit.

The $I = J = 1/2$ flavour multiplet contains the large N_c analogues of the neutron and proton. As long as the temperature of matter lies below the splitting between the baryon doublet and higher multiplets, *i. e.*, for T less than of order $1/N_c$, one can consider matter to consist of just the lowest doublet of baryons and the electron. Local charge neutrality and stability against β -decay and electron capture of cold matter

then requires two conditions on the Fermi energies

$$m_p E_F^p = m_e E_F^e, \quad \text{and} \quad E_F^n = E_F^p + E_F^e, \quad (10)$$

provided that the decay neutrinos escape from matter. Then writing $\epsilon = m_e/m_p \propto 1/N_c$, one finds that $E_F^p = \epsilon E_F^e$ and that $E_F^n \simeq E_F^e$. If the star has nucleon number A , then one finds the proton number to be $Z \propto A/N_c^{3/2}$. In the limit a neutron star can consist of only neutrons and electrons, the latter also being neutral due to the scaling of the electron charge in the 't Hooft limit. Interestingly, magnetic field effects can be interesting in this limit only if magnetic field strengths are of order $\sqrt{N_c}$. BNS mergers which raise the temperature of matter by more than order $1/N_c$ would then excite the full ladder of quark model baryons and possibly cross over into a state with quark matter.

6 Acknowledgements

I would like to thank Bastian Brandt, Heng-Tong Ding and Gergeli Endrödi for useful discussions and critical readings of the manuscript.

References

- [1] M. J. Buckingham, Phase Transitions and Critical Phenomena, Vol 2, ed. C. Domb and M. S. Green, Academic Press (1972)
- [2] L. G. Yaffe and B. Svetitsky, Phys. Rev. D **26**, 963 (1982)
- [3] J. Polonyi and K. Szlachanyi, Phys. Lett. B **110**, 395-398 (1982)
- [4] S. Datta and S. Gupta, Phys. Rev. D **80**, 114504 (2009) [arXiv:0909.5591 [hep-lat]].
- [5] M. G. Alford, J. Berges and K. Rajagopal, Nucl. Phys. B **558**, 219-242 (1999) [arXiv:hep-ph/9903502 [hep-ph]].
- [6] F. R. Brown, F. P. Butler, H. Chen, N. H. Christ, Z. h. Dong, W. Schaffer, L. I. Unger and A. Vaccarino, Phys. Rev. Lett. **65**, 2491-2494 (1990) doi:10.1103/PhysRevLett.65.2491
- [7] F. Cuteri, O. Philipsen and A. Sciarra, JHEP **11**, 141 (2021) [arXiv:2107.12739 [hep-lat]].
- [8] G. Endrodi, Prog. Part. Nucl. Phys. **141**, 104153 (2025) [arXiv:2406.19780 [hep-lat]].
- [9] L. McLerran and R. D. Pisarski, Nucl. Phys. A **796**, 83-100 (2007) [arXiv:0706.2191 [hep-ph]].

- [10] S. Datta and S. Gupta, Phys. Rev. D **82**, 114505 (2010) [arXiv:1006.0938 [hep-lat]].
- [11] B. Lucini and M. Panero, Phys. Rept. **526**, 93-163 (2013) [arXiv:1210.4997 [hep-th]].
- [12] L. McLerran and S. Reddy, Phys. Rev. Lett. **122**, no.12, 122701 (2019) [arXiv:1811.12503 [nucl-th]].
- [13] A. Cherman, S. Sen, M. Unsal, M. L. Wagman and L. G. Yaffe, Phys. Rev. Lett. **119**, no.22, 222001 (2017) [arXiv:1706.05385 [hep-th]].
- [14] S. Aoki *et al.* [JLQCD], Phys. Rev. D **103**, no.7, 074506 (2021) [arXiv:2011.01499 [hep-lat]].
- [15] R. V. Gavai, M. E. Jaensch, O. Kaczmarek, F. Karsch, M. Sarkar, R. Shanker, S. Sharma, S. Sharma and T. Ueding, Phys. Rev. D **111**, no.3, 034507 (2025) [arXiv:2411.10217 [hep-lat]].
- [16] Z. Fodor, A. Y. Kotov, T. G. Kovacs and K. K. Szabo, [arXiv:2503.22243 [hep-lat]].
- [17] S. Mondal, S. Mukherjee and P. Hegde, Phys. Rev. Lett. **128**, no.2, 022001 (2022) [arXiv:2106.03165 [hep-lat]].
- [18] S. Mitra, P. Hegde and C. Schmidt, Phys. Rev. D **106**, no.3, 034504 (2022) [arXiv:2205.08517 [hep-lat]].
- [19] C. R. Allton, S. Ejiri, S. J. Hands, O. Kaczmarek, F. Karsch, E. Laermann, C. Schmidt and L. Scorzato, Phys. Rev. D **66**, 074507 (2002) [arXiv:hep-lat/0204010 [hep-lat]].
- [20] J. Polonyi, Central Eur. J. Phys. **1**, 1-71 (2003) [arXiv:hep-th/0110026 [hep-th]].
- [21] W. Metzner, M. Salmhofer, C. Honerkamp, V. Meden and K. Schonhammer, Rev. Mod. Phys. **84**, 299 (2012) [arXiv:1105.5289 [cond-mat.str-el]].
- [22] N. Dupuis, L. Canet, A. Eichhorn, W. Metzner, J. M. Pawłowski, M. Tissier and N. Wschebor, Phys. Rept. **910**, 1-114 (2021) [arXiv:2006.04853 [cond-mat.stat-mech]].
- [23] F. Gao and J. M. Pawłowski, Phys. Lett. B **820**, 136584 (2021) [arXiv:2010.13705 [hep-ph]].
- [24] R. D. Pisarski and F. Wilczek, Phys. Rev. D **29**, 338-341 (1984)
- [25] Y. Aoki, G. Endrodi, Z. Fodor, S. D. Katz and K. K. Szabo, Nature **443**, 675-678 (2006) [arXiv:hep-lat/0611014 [hep-lat]].

- [26] A. Bazavov *et al.* [HotQCD], Phys. Lett. B **795** (2019), 15-21 [arXiv:1812.08235 [hep-lat]].
- [27] S. Borsanyi, Z. Fodor, J. N. Guenther, R. Kara, S. D. Katz, P. Parotto, A. Pasztor, C. Ratti and K. K. Szabo, Phys. Rev. Lett. **125** (2020) no.5, 052001 [arXiv:2002.02821 [hep-lat]].
- [28] H. T. Ding *et al.* [HotQCD], Phys. Rev. Lett. **123**, no.6, 062002 (2019) [arXiv:1903.04801 [hep-lat]].
- [29] B. B. Brandt, O. Philipsen, M. Cè, A. Francis, T. Harris, H. B. Meyer and H. Wittig, PoS **CD2018**, 055 (2019) [arXiv:1904.02384 [hep-lat]].
- [30] M. Bresciani, M. Dalla Brida, L. Giusti and M. Pepe, PoS **LATTICE2023**, 192 (2024) [arXiv:2312.11009 [hep-lat]].
- [31] S. P. Klevansky, Rev. Mod. Phys. **64**, 649-708 (1992)
- [32] J. Gasser and H. Leutwyler, Annals Phys. **158**, 142 (1984)
- [33] E. V. Shuryak and J. J. M. Verbaarschot, Nucl. Phys. A **560**, 306-320 (1993) [arXiv:hep-th/9212088 [hep-th]].
- [34] J. Gasser and H. Leutwyler, Phys. Lett. B **188**, 477-481 (1987)
- [35] P. Gerber and H. Leutwyler, Nucl. Phys. B **321**, 387-429 (1989)
- [36] S. Gupta and R. Sharma, Phys. Rev. D **97**, no.3, 036025 (2018) [arXiv:1710.05345 [hep-ph]].
- [37] S. Gupta, R. Sharma and P. Sen, [arXiv:2511.00409 [hep-lat]].
- [38] D. T. Son and M. A. Stephanov, Phys. Rev. D **66**, 076011 (2002) [arXiv:hep-ph/0204226 [hep-ph]].
- [39] S. Gupta and R. Sharma, Int. J. Mod. Phys. A **35**, no.33, 2030021 (2020) [arXiv:2006.16626 [hep-ph]].
- [40] A. Barducci, R. Casalbuoni, G. Pettini and R. Gatto, Phys. Rev. D **49**, 426-436 (1994)
- [41] A. M. Halasz, A. D. Jackson, R. E. Shrock, M. A. Stephanov and J. J. M. Verbaarschot, Phys. Rev. D **58**, 096007 (1998) [arXiv:hep-ph/9804290 [hep-ph]].
- [42] M. A. Stephanov, K. Rajagopal and E. V. Shuryak, Phys. Rev. Lett. **81**, 4816-4819 (1998) [arXiv:hep-ph/9806219 [hep-ph]].

- [43] S. Datta, R. V. Gavai and S. Gupta, Phys. Rev. D **95**, no.5, 054512 (2017) [arXiv:1612.06673 [hep-lat]].
- [44] D. A. Clarke, P. Dimopoulos, F. Di Renzo, J. Goswami, C. Schmidt, S. Singh and K. Zambello, [arXiv:2405.10196 [hep-lat]].
- [45] F. Karsch, E. Laermann and A. Peikert, Nucl. Phys. B **605**, 579-599 (2001) [arXiv:hep-lat/0012023 [hep-lat]].
- [46] R. V. Gavai and S. Gupta, Phys. Rev. D **66**, 094510 (2002) [arXiv:hep-lat/0208019 [hep-lat]].
- [47] D. T. Son and M. A. Stephanov, Phys. Rev. Lett. **86**, 592-595 (2001) [arXiv:hep-ph/0005225 [hep-ph]].
- [48] B. B. Brandt, G. Endrodi and S. Schmalzbauer, Phys. Rev. D **97**, no.5, 054514 (2018) [arXiv:1712.08190 [hep-lat]].
- [49] B. B. Brandt, F. Cuteri and G. Endrodi, JHEP **07**, 055 (2023) [arXiv:2212.14016 [hep-lat]].
- [50] J. B. Kogut and D. K. Sinclair, Phys. Rev. D **66**, 034505 (2002) [arXiv:hep-lat/0202028 [hep-lat]].
- [51] R. V. Gavai and S. Gupta, Phys. Rev. D **68**, 034506 (2003) [arXiv:hep-lat/0303013 [hep-lat]].
- [52] R. V. Gavai and S. Gupta, Phys. Rev. D **71**, 114014 (2005) [arXiv:hep-lat/0412035 [hep-lat]].
- [53] S. Gupta and R. Sharma, PoS **CPOD2014**, 011 (2015) [arXiv:1503.03206 [hep-lat]].
- [54] J. A. Lipa, D. R. Swanson, J. A. Nissen, T. C. P. Chui and U. E. Israelsson, Phys. Rev. Lett. **76**, 944-947 (1996)
- [55] R. Abbott *et al.* [NPLQCD], Phys. Rev. Lett. **134**, no.1, 1 (2025) [arXiv:2406.09273 [hep-lat]].
- [56] A. Sedrakian, Prog. Part. Nucl. Phys. **58**, 168-246 (2007) [arXiv:nucl-th/0601086 [nucl-th]].
- [57] N. K. Glendenning, Phys. Rept. **342**, 393-447 (2001)
- [58] G. Watanabe, K. Iida and K. Sato, Nucl. Phys. A **676**, 455-473 (2000) [erratum: Nucl. Phys. A **726**, 357-365 (2003)] [arXiv:astro-ph/0001273 [astro-ph]].

- [59] T. Maruyama, T. Tatsumi, D. N. Voskresensky, T. Tanigawa and S. Chiba, Phys. Rev. C **72**, 015802 (2005) [arXiv:nucl-th/0503027 [nucl-th]].
- [60] S. S. Avancini, L. Brito, J. R. Marinelli, D. P. Menezes, M. M. W. de Moraes, C. Providencia and A. M. Santos, Phys. Rev. C **79**, 035804 (2009) [arXiv:0812.3170 [nucl-th]].
- [61] J. Berges and K. Rajagopal, Nucl. Phys. B **538**, 215-232 (1999) [arXiv:hep-ph/9804233 [hep-ph]].
- [62] K. Rajagopal and F. Wilczek, [arXiv:hep-ph/0011333 [hep-ph]].
- [63] M. G. Alford, K. Rajagopal, S. Reddy and F. Wilczek, Phys. Rev. D **64**, 074017 (2001) [arXiv:hep-ph/0105009 [hep-ph]].
- [64] C. K. Chow and T. M. Yan, Phys. Rev. D **53**, 5105-5107 (1996) [arXiv:hep-ph/9512243 [hep-ph]].
- [65] R. Shrock, Phys. Rev. D **53**, 6465-6476 (1996) [arXiv:hep-ph/9512430 [hep-ph]].
- [66] G. 't Hooft, Nucl. Phys. B **72**, 461 (1974)
- [67] E. Witten, Nucl. Phys. B **160**, 57-115 (1979)
- [68] J. L. Gervais and B. Sakita, Phys. Rev. Lett. **52**, 87 (1984)
- [69] J. L. Gervais and B. Sakita, Phys. Rev. D **30**, 1795 (1984)
- [70] E. E. Jenkins, Phys. Lett. B **315**, 441-446 (1993) [arXiv:hep-ph/9307244 [hep-ph]].
- [71] M. Cheng, N. H. Christ, S. Datta, J. van der Heide, C. Jung, F. Karsch, O. Kaczmarek, E. Laermann, R. D. Mawhinney and C. Miao, *et al.* Phys. Rev. D **74**, 054507 (2006) [arXiv:hep-lat/0608013 [hep-lat]].